HAL
open science

Remote-sensing measurements in the polar vortex: Comparison to in situ observations and implications for the simultaneous retrievals and analysis of the NO2 and OClO species

Gwenaël Berthet, Jean-Baptiste Renard, Valéry Catoire, Michel Chartier, Claude Robert, Nathalie Huret, F. Coquelet, Q. Bourgeois, Emmanuel D. Rivière, Brice Barret, et al.

To cite this version:

Gwenaël Berthet, Jean-Baptiste Renard, Valéry Catoire, Michel Chartier, Claude Robert, et al.. Remote-sensing measurements in the polar vortex: Comparison to in situ observations and implications for the simultaneous retrievals and analysis of the NO2 and OClO species. Journal of Geophysical Research: Atmospheres, 2007, 112 (D21), pp.D21310. 10.1029/2007JD008699 . hal-00561485

HAL Id: hal-00561485

https://hal.science/hal-00561485

Submitted on 25 Oct 2016

HAL is a multi-disciplinary open access archive for the deposit and dissemination of scientific research documents, whether they are published or not. The documents may come from teaching and research institutions in France or abroad, or from public or private research centers.

L'archive ouverte pluridisciplinaire **HAL**, est destinée au dépôt et à la diffusion de documents scientifiques de niveau recherche, publiés ou non, émanant des établissements d'enseignement et de recherche français ou étrangers, des laboratoires publics ou privés.

Remote-sensing measurements in the polar vortex: Comparison to in situ observations and implications for the simultaneous retrievals and analysis of the NO_2 and OClO species

G. Berthet,[1] J.-B. Renard,[1] V. Catoire,[1] M. Chartier,[1] C. Robert,[1] N. Huret,[1] F. Coquelet,[1] Q. Bourgeois,[1] E. D. Rivière,[2] B. Barret,[3] F. Lefèvre,[4] and A. Hauchecorne[4]

Received 24 March 2007; revised 18 July 2007; accepted 3 August 2007; published 13 November 2007.

[1] Nighttime remote-sensing balloon observations conducted by the SALOMON instrument in the arctic polar vortex in January 2006 reveal high amounts of stratospheric NO_2 in the lower stratosphere similarly to previously published profiles. NO_2 concentration enhancements are also present in the vertical profiles observed by the GOMOS instrument on board the Envisat satellite and obtained coincidently to the balloon measurements. Such quantities are not present in in situ observations obtained by the SPIRALE instrument in similar geophysical conditions. While OClO amounts are acceptably reproduced by Chemistry Transport Model (CTM) calculations, NO_2 simulated values are well below the observed quantities. The examination of the slant column densities of NO_2 obtained at float altitude highlights unexpected strong enhancements with respect to the elevation angle and displacement of the balloon. It is shown that these fluctuations result from NO_2 spatial inhomogeneities located above the balloon float altitude. Potential vorticity maps reveal the presence of midlatitude NO_2-rich air in the upper stratosphere or lower mesosphere as a result of the perturbed dynamical situation of the vortex. The presence of spatial inhomogeneities crossed by the lines of sight leads to artificial high concentration values of NO_2 in the vertical profile retrieved from the slant column densities assuming spatial homogeneity. A direct implication is that the differences previously observed between measurements of NO_2 and OClO and model results are probably mostly due to the improper inversion of NO_2 in the presence of perturbed dynamical conditions or when mesospheric NO_x production events occur. The dynamical situation will have to be systematically analyzed in future studies involving remote-sensing observations.

Citation: Berthet, G., et al. (2007), Remote-sensing measurements in the polar vortex: Comparison to in situ observations and implications for the simultaneous retrievals and analysis of the NO_2 and OClO species, *J. Geophys. Res.*, *112*, D21310, doi:10.1029/2007JD008699.

1. Introduction

[2] Remote-sensing measurements from spectrometers on board various platforms (balloons, aircrafts, satellites) have been used for decades to retrieve slant column density (hereafter SCD) values or vertical profiles of the stratospheric chemical compounds. Several studies have focused on the interactions between nitrogen and halogen species which are of primary importance for polar ozone chemistry. Active chlorine species are indeed involved in the ozone destroying catalytic cycles whereas nitrogen species act in the deactivation mechanisms of chlorine. Recent work has particularly centered on the NO_2 and OClO species from simultaneous observations by balloon-borne UV-visible spectrometers [*Rivière et al.*, 2002, 2004].

[3] NO_2 and OClO are chemically linked through the following reactions. OClO is predominantly formed at sunset in the winter polar vortex through one channel of the reaction of ClO with BrO:

$$BrO + ClO \rightarrow OClO + Br \quad (1a)$$

$$\rightarrow ClOO + Br \quad (1b)$$

$$\rightarrow BrCl + O_2 \quad (1c)$$

[1]Laboratoire de Physique et Chimie de l'Environnement, CNRS and Université d'Orléans, Orléans, France.
[2]Groupe de Spectrométrie Moléculaire et Atmosphérique, Université de Reims and CNRS, Reims, France.
[3]Laboratoire d'Aérologie, Observatoire de Midi-Pyrénées, Toulouse, France.
[4]Service d'Aéronomie, Institut Pierre-Simon Laplace, Paris, France.

Copyright 2007 by the American Geophysical Union.
0148-0227/07/2007JD008699

[4] The production of OClO is assumed to be reduced by the two following reactions involving NO_2:

$$ClO + NO_2 + M \rightarrow ClONO_2 + M \quad (2)$$

$$BrO + NO_2 + M \rightarrow BrONO_2 + M \quad (3)$$

[5] From the studies mentioned above it clearly appears that models are not able to reproduce simultaneously the various profiles of NO_2 and OClO measured in the arctic polar vortex. *Rivière et al.* [2002] have in particular reported high observed quantities of NO_2 on 23 January 2000 at altitude levels where full denoxification ($NO_x = NO + NO_2$) is simulated. Possible sources of NO_2 have been invoked to explain the large missing quantities of NO_2 in the model calculations. However, such quantities of NO_2 lead unequivocally to low simulated amounts of OClO due to reactions (2) and (3). *Rivière et al.* [2004] raised the possibility of formation of isomers of $ClONO_2$ and $BrONO_2$ (resulting in a decrease of rate constants of reactions (2) and (3) and an increase of the modeled amounts of OClO) to improve the comparisons between observations and simulations of OClO and NO_2. *Canty et al.* [2005] have obtained a finer agreement between model results and the balloon observations of OClO than did *Rivière et al.* [2002] for the observational case of 23 January 2000. Considering denoxified conditions, they have actually ignored the observed high amounts of NO_2 which are in total disagreement with the currently known polar chemistry, an assumption based on the very low levels of NO observed in situ by a chemiluminescence instrument on board the ER-2 [*Gao et al.*, 1997]. This has been achieved by constraining their model with measurements of active bromine and chlorine, increasing one of the branching ratios of the ClO + BrO reaction to a value close to the uncertainty upper limit given by 2002 JPL kinetics [*Sander et al.*, 2003] and taking into account various sources of uncertainties in the model. In particular, *Canty et al.* [2005] have underlined the importance of accurate knowledge of air parcel trajectories for correct modeling of OClO.

[6] Recently, *Swartz et al.* [2006] have pointed out that spatial inhomogeneities in the line-of-sight measurements from aircraft are likely to affect the retrieval of vertical profiles of species like ozone. Therefore a doubt remains regarding the NO_2 quantities measured in the polar vortex, especially in the lower stratosphere where significant amounts of NO_2 have been recurrently observed by remote-sensing balloon-borne instruments [*Sen et al.*, 1998; *Payan et al.*, 1999; *Wetzel et al.*, 2002; *Rivière et al.*, 2002; *Berthet et al.*, 2003]. A balloon campaign was then conducted in Kiruna (Sweden, 67.9°N, 22.1°E) in the Northern Hemisphere (NH) polar vortex in theoretically denoxified conditions to investigate the NO_2 quantities derived from such measurements by comparing them to in situ observations and to model calculations. The observations were made during the night allowing us to get rid of species concentration variations as a function of local time which generally have to be corrected for solar occultation measurements.

2. Instruments

[7] Stratospheric profiles were measured by the SALOMON (SALOMON is a French acronym for Spectroscopie d'Absorption Lunaire pour l'Observation des Minoritaires Ozone et NO_x) and SPIRALE (French acronym for Spectroscopie Infrarouge d'Absorption par Lasers Embarqués) balloon-borne instruments used routinely at all latitudes, in particular as part of European and satellite validation campaigns. The performance characteristics of the SALOMON instrument and data reduction method have been described in detail by *Renard et al.* [2000] and *Berthet et al.* [2003]. A detailed description of the instrumental characteristics of SPIRALE and of its operating mode is given by *Moreau et al.* [2005].

[8] SALOMON performs nighttime remote-sensing measurements of NO_2 and OClO from their UV-visible absorption bands using the well-established DOAS (Differential Optical Absorption Spectroscopy) technique [e.g., *Platt*, 1994]. Note that to our knowledge, no other instrument conducts measurements in the UV-visible wavelength range from a balloon at night. The measurement is self-calibrated since no assumption concerning the response of the instrument is needed. The spectrometer does not suffer from any kind of mechanical deformations during the moon pointing procedure. The instrument is thermally insulated and thus not affected by external temperature variations. Direct moon spectra are collected and recorded on board the azimuth-elevation-controlled SALOMON gondola. The spectra cover the 340–700 nm wavelength domain and are sampled at 0.34 nm per pixel. At the balloon float altitude a reference spectrum is recorded when the moon is well above the gondola horizon. This spectrum is carefully chosen so that it contains minimized species absorption features. Owing to the high moon-pointing accuracy, two specific geometries of observation can be carried out to record the raw spectra: (1) at float altitude while the moon sets or rises below the gondola horizon (typical occultation configuration) or (2) during the balloon ascent and at float altitude with the moon located above the gondola horizon (positive elevation angles typically from 0 to 30°). The schematic view of the geometry of observation during balloon ascent and at float is presented in Figure 1. Dividing the raw spectra with the reference spectrum gives the transmission spectra highlighting the atmospheric species absorption bands. NO_2 and OClO SCDs are determined respectively over the 420–510 and 340–420 nm spectral ranges by least squares fits using the University of Bremen high resolution absorption cross-sections measured at University of Bremen (data available at http://www.iup.physik.uni-bremen.de/gruppen/molspec/index.html). Vertical profiles of the species are obtained by mathematical inversion of the SCD profile using a least squares method based upon the common assumptions of spherical symmetry and homogeneity of the stratospheric layers. Note that for an ascent flight configuration with positive moon elevation angles, Figure 1 represents the stratospheric layers (grey shaded area) crossed by the lines of sight used to retrieve the vertical profile. Concentration error bars are given by three standard deviations in the least squares fit. SALOMON observations were conducted on 16 January 2006 between 1645 UT and 2100 UT in the 14–34 km altitude range inside the polar vortex during the ascent of the balloon and at float altitude with the moon above the gondola horizon as described in Figure 1.

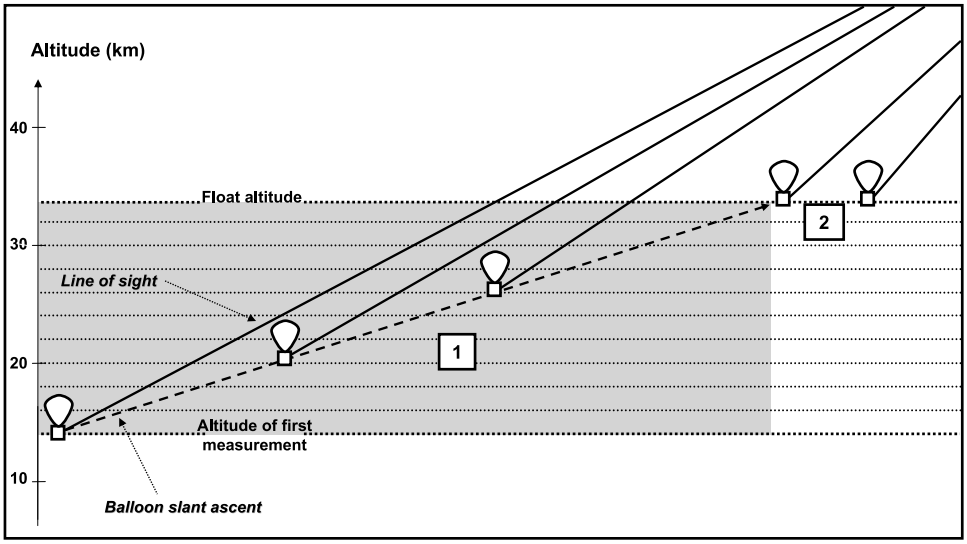

Figure 1. Schematic view of the geometry of observation for SALOMON measurements performed during ascent (1) and at float (2). The grey-shaded area encompasses the stratospheric layers sounded by the infinite lines of sight during ascent and corresponding to the vertical profile retrieved after mathematical inversion of the slant column densities. Homogeneity of these layers is assumed for the retrieval of the concentration vertical profile. Observations conducted at float provide slant column densities varying through increase of moon elevation and horizontal displacement of the balloon.

[9] SPIRALE is dedicated to in situ observations of NO_2 and various long-lived and short-lived chemical species from about 10 to 40 km with a vertical resolution of a few meters. It uses six tunable salt laser diodes in the mid-infrared domain (3 μm to 10 μm) where molecular line strengths are the greatest. The laser diodes are cooled and the beams are injected into a multipass Heriott cell located under the gondola and largely exposed to ambient air. The cell (3.5 m long) is deployed during the flight when pressure is lower than 300 hPa. The multiple reflections obtained between the two cell mirrors give a total optical path of 430.78 m. Species concentrations are retrieved from direct infrared absorption, by fitting experimental spectra with spectra calculated using HITRAN 2004 database [*Rothman et al.*, 2005] in the micro-window 1598.4–1598.9 cm^{-1}. The global uncertainties for NO_2 have been assessed by taking into account the random errors and the systematic errors, and combining them as the square root of their quadratic sum. In brief, there are two important sources of random errors: (1) the fluctuations of the laser background emission signal and (2) the signal-to-noise ratio. These error sources are the main contributions for NO_2 giving a total uncertainty of 30% at the lower altitudes (around 17 km), reduced to 20% around 24 km, and even to 6% above 24 km. With respect to the above errors, systematic errors on spectroscopic data (essentially molecular line strength and pressure broadening coefficients) are considered to be negligible. The SPIRALE flight occurred on 20 January 2006 between 1800 UT and 1950 UT with profiles obtained in the vortex between 17 and 27.2 km under similar time and geophysical conditions as SALOMON for appropriate comparisons.

[10] GOMOS (acronym for Global Ozone Monitoring by Occultation of Stars) on board the European satellite Envisat launched in March 2002 is a space instrument using for the first time a stellar occultation technique to observe stratospheric and mesospheric species that present absorption lines in the UV-visible and near infra red domains (248–942 nm) [*Bertaux et al.*, 2004; *Hauchecorne et al.*, 2005]. The reference star spectrum is recorded at the beginning of the occultation outside the atmosphere then occultation spectra are recorded during the set of the star. As those of SALOMON, the GOMOS measurements can be considered self-calibrated. Dedicated to provide a climatology of species involved in the ozone photochemistry, GOMOS provides in particular global NO_2 observations with a vertical sampling of about 1.5 km from about 135 km down to the lower stratosphere. The NO_2 data presented in this study correspond to version V5.0 of the algorithms. *Marchand et al.* [2004] have analyzed the self-consistency of GOMOS NO_2 data using chemical data assimilation and have found no evidence for a bias. The validation work of *Renard et al.* [2007] shows that the GOMOS individual profiles of NO_2 obtained at midlatitude and high latitude compare reasonably well with balloon observations in the middle stratosphere, at least statistically, both in terms of altitudes and concentration values. We therefore assume that GOMOS individual profiles of NO_2 can be used for specific comparisons with balloon observations. For such analysis the collocation criteria between GOMOS and balloon observations are typically less than 500 km in the same physical conditions and less than 3 hours. This was the case for the two balloon flights studied here.

3. Model Experiment

[11] The three-dimensional simulations presented here have been performed with the REPROBUS (Reactive

Processes Ruling the Ozone Budget in the Stratosphere) Chemical Transport Model (CTM) [*Lefèvre et al.*, 1994, 1998] which has been extensively used in previous studies of the stratospheric chemistry especially at high latitudes [e.g., *Hoppel et al.*, 2002; *Ricaud et al.*, 2005]. The model computes the evolution of 55 species through about 160 photolytic gas-phase and heterogeneous reactions with a time step of 15 min in the present study. 40 species or chemical families, typically long-lived tracers, are transported by a semi-Lagrangian code. The kinetics of all chemical reactions is taken from the 2002 JPL recommendation [*Sander et al.*, 2003], except for the photolysis rate of Cl_2O_2 taken from *Burkholder et al.* [1990] with a wavelength extrapolation to 450 nm following the work of *Stimpfle et al.* [2004]. The laboratory measurements of photodissociation cross-sections of HO_2NO_2 both in the UV [*Knight et al.*, 2002] and in the near IR [*Roehl et al.*, 2002] have been included in the photodissociation calculations.

[12] We make use here of an improved version of REPROBUS including an explicit description of the inorganic bromine (Br_y) budget. The time-dependent sources and chemistries of CH_3Br and halons (H-1211, H-1301, H-2402) are calculated, as well as the additional contribution of bromine very short-lived species [*Salawitch et al.*, 2005], represented in the form of equivalent CH_2Br_2 in the model. This additional bromine contribution is set to a value of 6 pptv in REPROBUS compared to the 4–8 pptv range suggested by *Salawitch et al.* [2005]. This leads to a stratospheric inorganic bromine burden of about 23 pptv calculated by REPROBUS. Monthly varying H_2SO_4 fields leading to the formation of liquid aerosols in the CTM are computed from the outputs of a two-dimensional model long-term simulation which takes into account impacts of volcanic eruptions [*Bekki et al.*, 1996]. The heterogeneous chemistry module used in the present simulation includes reactions on binary and ternary liquid aerosols, as well as on water-ice particles. The composition of liquid aerosols is calculated analytically [*Carslaw et al.*, 1995]. The ice particles are assumed to incorporate HNO_3 in the form of nitric acid trihydrate (NAT) described by a bimodal size distribution based on the scheme of *Davies et al.* [2002].

[13] In the present study REPROBUS was integrated from April 2002 to January 2006. The model extends from the surface up to 0.1 hPa on 42 vertical levels resulting in a vertical resolution of about 1 km in the lower stratosphere. The horizontal resolution is 2° latitude by 2° longitude. Species were initialized from the outputs of a long-term simulation (1958–2003) of a two-dimensional model previously used in a variety of atmospheric studies [e.g., *Bekki et al.*, 1994; *Bekki and Law*, 1997]. REPROBUS was driven by the European Centre for Medium-Range Weather Forecast (ECMWF) meteorological data (temperature, ground pressure and three-dimensional winds). The simulation was forced using 3-hourly ECMWF meteorological data constructed from operational analysis and forecasts instead of using common 6-hourly operational analysis. This appears to result in a more accurate modeling of NO_y species as shown by *Berthet et al.* [2006] for NO_2 and HNO_3.

4. Results and Discussion

4.1. OClO

[14] The vertical profile of nighttime OClO concentrations (Figure 2) was measured on 16 January 2006 by SALOMON during the balloon ascent inside the vortex. PSCs were observed above Kiruna over the previous days with cold temperatures recorded and are indicative of the onset of chlorine activation processes. This gives rise to the amounts of OClO measured by SALOMON on 16 January keeping in mind that OClO is only a qualitatively good indicator of chlorine activation [*Sessler et al.*, 1995].

[15] Figure 2 shows a comparison of the observed OClO concentrations to the REPROBUS model calculations. Model profiles were extracted during the simulation to coincide to the varying time and locations of the balloon measurements ranging respectively from 1645 UT to 2100 UT and from 68°N–21°E to 69°N–25°E. The set of these calculated profiles (represented by the shaded area in the plot) thus accounts for the time evolution of the species and considers all the model grid points enclosing the observation positions. Overall, OClO concentrations are acceptably reproduced by the model using the chemical reaction rates of the JPL compilation [*Sander et al.*, 2003] and the ECMWF meteorological fields taking into account both the error bars and the dispersion of the calculated profiles. This result can be considered to be in agreement with the works of *Rivière et al.* [2002] and *Canty et al.* [2005] though a model-measurement discrepancy is observed for the two concentration values in the lower part of the vertical profile (Figure 2). It is out of the scope of this paper to perform model sensitivity tests to reduce this discrepancy as thoroughly done by *Canty et al.* [2005] but possible explanations can be found. These authors show that nighttime OClO in the Arctic vortex depends on three major factors: the air mass history during the last sunrise and sunset transitions, the branching ratios of the reaction BrO + ClO, and the amounts of BrO_x (BrO + BrCl). Accurate knowledge of these factors is therefore required for an appropriate modeling of nighttime OClO. First, air parcel trajectories are considered to be better simulated in the REPROBUS CTM using 3-hourly ECMWF winds following the results of *Berthet et al.* [2006] but uncertainties are most likely to remain in the details of air parcel history. Secondly, concerning the branching ratios of the reaction BrO + ClO, the yield of BrCl (reaction (1c)) is associated with a large uncertainty range in the 2002 JPL kinetics. *Canty et al.* [2005] have increased the BrCl yield to a value of 11% which is close to the upper limit of the uncertainty. This has resulted in a decrease of the nighttime OClO quantities calculated by an isentropic trajectory model in agreement with the SALOMON observations of 23 January 2000 presented in their study. In our case, we have chosen to compute the 7% value recommended by JPL since using this upper limit value would have led to a further difference with the SALOMON observations shown in Figure 2. Finally, nighttime OClO amounts are very sensitive to daytime BrO_x and to BrO quantities available in twilight

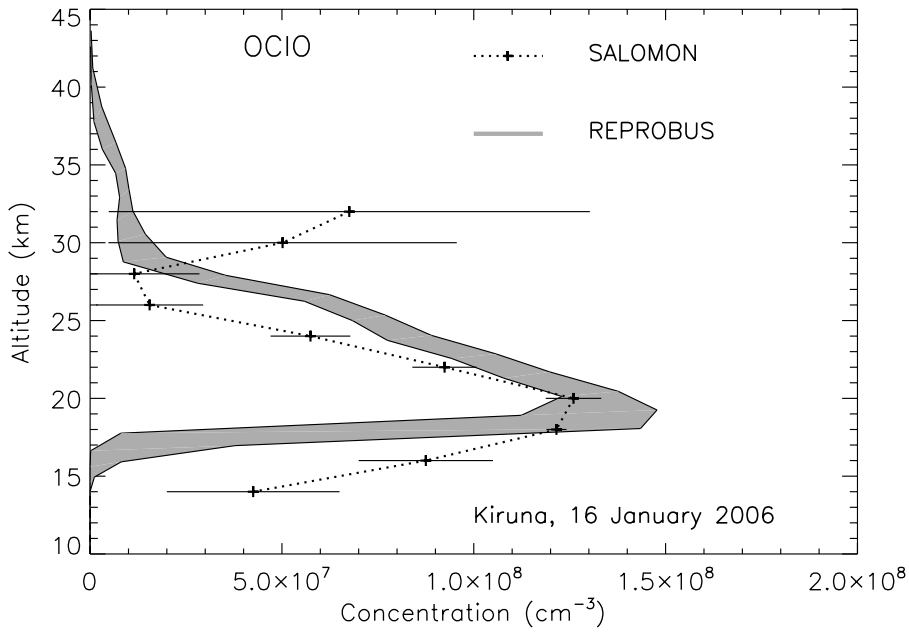

Figure 2. Vertical profile of OClO concentrations measured on 16 January 2006 by SALOMON in the polar night inside the vortex during the balloon ascent. The observed profile is compared to the set of profiles simulated by REPROBUS (expressed by the shaded area in the plot) at the time and positions enclosing the balloon observations ranging from 1645 UT to 2100 UT and from 68°N–21°E to 69°N–25°E.

rather than to the levels of ClO_x (ClO + 2 × ClOOCl). The work of *Salawitch et al.* [2005] strongly suggests that the amount of stratospheric reactive bromine is underestimated in models. Following the results of *Salawitch et al.* [2005] and as stated in section 3, the 6 pptv additional bromine contribution we have chosen to compute in the upgraded version of REPROBUS could be still underestimated (an upper limit of 8 pptv is suggested by *Salawitch et al.* [2005]) to correspond to the real amount of stratospheric inorganic bromine. An underestimation of BrO_x computed in REPROBUS would result in an underestimation of the modeled quantities of OClO as shown by the sensitivity test done by *Canty et al.* [2005] at 59 hPa (about 18 km). In the case presented in Figure 2 computing REPROBUS without including the additional bromine contribution results in a decrease of simulated amounts of OClO of about 8% around 20 km (but insignificant below about 18 km) demonstrating the sensitivity of this species to levels of active bromine at least at some altitude levels (not shown). BrO observations suffer from significant uncertainties and no measurements of BrCl are currently available. On the basis of these facts it is difficult to constrain the models with very accurate levels of BrO_x necessary to simulate more confidently nighttime OClO. Note that a better knowledge of BrO quantities would help for a more accurate modeling of OClO through a better determination of the BrCl yield from reaction (1c).

[16] The maximum concentration value of OClO observed at 20 km (1.26×10^8 cm^{-3}) corresponds to a mixing ratio of 75 pptv. From such a typical value of OClO low amounts of NO_2 are theoretically expected at these altitude levels.

4.2. NO_2

[17] Figure 3 presents the NO_2 concentration profile from SALOMON observations during the balloon ascent. A NO_2 enhancement is clearly visible below 20 km as already observed in the polar vortex in previous campaigns. GOMOS observations obtained at comparable time (2000 UT) and location (around 400 km from SALOMON position; 71.8°N–72.2°N; 20.2°E–21.8°E; 2000UT, time differences of 1.5–3.0 hours) with the SALOMON profile are presented and also reveal a secondary maximum below 20 km. The altitudes of the NO_2 maximums are in rather good agreement between the two instruments but SALOMON provides higher concentration values between 18 and 24 km and between 26 and 28 km. Between 14 and 24 km, note the presence of an oscillation in the GOMOS profile from positive to negative concentration values. Another maximum is present in GOMOS observations around 38 km. Due to the diurnal variation of NO_2 the temporal differences between GOMOS and SALOMON may be responsible at least for parts of the deviations between the two instruments.

[18] In Figure 3 the SALOMON observations of NO_2 have been compared to a set of profiles simulated by REPROBUS coinciding to the times and locations of the balloon measurements during ascent. Simulated concentrations are significantly below the SALOMON observed values between 20 and 30 km. In particular, as theoretically expected, denoxified conditions are modeled between 20 and 24 km with values very close to zero compared to measured concentrations of $4.2–1.5 \times 10^8$ cm^{-3} (250–170 pptv). Below 20 km the SALOMON profile depicts large error bars but NO_2 amounts are shown to be higher than the simulation. The concentration values of NO_2 observed by GOMOS and calculated by REPROBUS are of the same amplitude above 31 km, in particular for the secondary peak around 38 km.

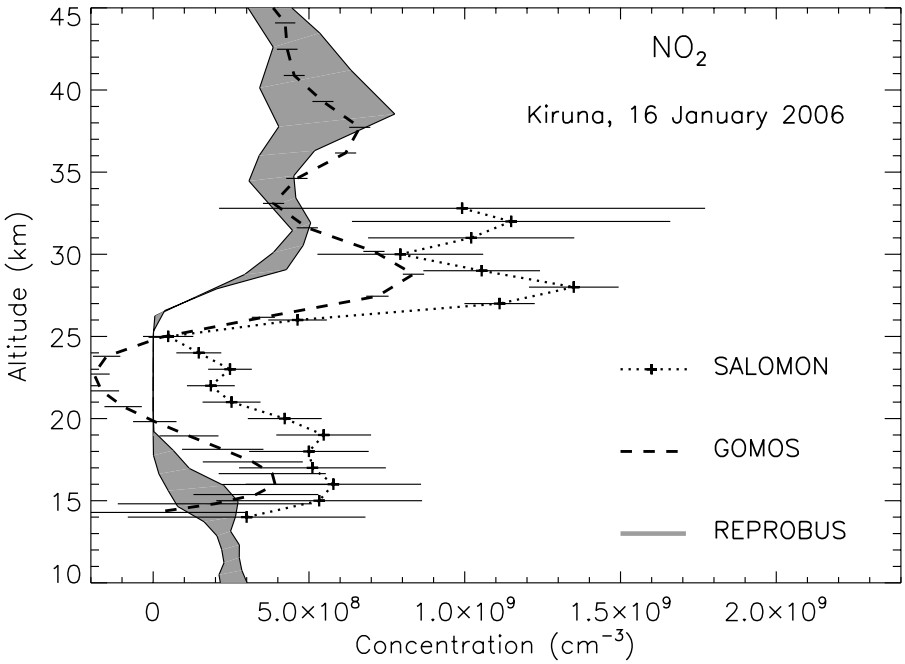

Figure 3. Vertical profile of NO_2 from nighttime observations of SALOMON inside the polar vortex on 16 January 2006 (1645–2100 UT). The profile is compared to the GOMOS/Envisat measurements available close to the balloon observations. The results of the REPROBUS simulation set (expressed by the vertical shaded area in the plot) at the time and positions enclosing the balloon observations are presented.

[19] The SPIRALE instrument was launched inside the polar vortex four days after SALOMON. The conditions of measurements are similar to those of SALOMON in terms of time and vortex conditions. In addition, the degree of chlorine activation computed by REPROBUS in the lower stratosphere is around 70% for both flights. The SPIRALE in situ profile of NO_2 was obtained between 1800 UT and 1950 UT (Figure 4) in the 17–27.2 km altitude range at almost constant latitude-longitude position since the balloon remained close to 67.7°N–21.6°E all along the ascent. Comparisons with GOMOS observations (about 500 km from SPIRALE position; 71.6°N–72.2°N; 21.3°E–22.2°E; 1940 UT, time differences up to 1.5 hours) and REPROBUS calculations (taking into account the variation of NO_2 during the measurement as in Figure 3) are also presented.

[20] In Figure 4 below 23 km SPIRALE measurements show denoxification with NO_2 concentrations close to zero (accounting for error bars). Surprisingly, this result totally differs from the SALOMON observations presented in Figure 3. One can note that GOMOS observations shown in Figure 3 reveal NO_2 amounts higher than zero around 23 km and below 18 km which is inconsistent with the results obtained by SPIRALE at these altitude levels. Unlike the REPROBUS-SALOMON comparisons excellent agreement is observed between the in situ profile and the model calculations below 23 km, both data revealing denoxified air masses as expected in the winter polar vortex conditions. Note that in Figure 4 there is no increase in the NO_2 concentrations calculated by REPROBUS between 15 and 19 km unlike the 16 January case (Figure 3). This feature seems to be due to the proximity of the vortex edge at these altitude levels for the 16 January case as revealed by the N_2O fields computed by REPROBUS (not shown).

[21] Above 23 km NO_2 concentrations measured by SPIRALE sharply increase with a gradient similar to the one in the SALOMON profile. The concentration maximum on the SPIRALE profile shows a good agreement with the maximum observed by SALOMON both in terms of altitude and amplitude taking into account the error bars (with for example concentrations of 1.2×10^9 and 1.1×10^9 cm^{-3} at 27 km for SPIRALE and SALOMON respectively). At all altitudes above 23 km a significant underestimation is clearly visible on the profile simulated by REPROBUS (as for the SALOMON-REPROBUS comparison), a discrepancy believed to be partly related to common deficiencies in the calculation of total NO_y already quantified for midlatitude conditions [*Berthet et al.*, 2006]. One could also argue about the impact of denitrification processes in the vortex not always satisfyingly calculated in CTMs (as can be seen for example in the work of *Ricaud et al.* [2005] from Odin/REPROBUS comparisons of HNO_3) and potentially reducing simulated active nitrogen through the link with HNO_3. Above 30 km the broad maximum present in GOMOS observations is also calculated by REPROBUS but with much higher NO_2 amounts in the simulation.

[22] From the analysis described above two points appear to be important. First, the analysis of the vertical profiles observed by SALOMON points out another case of simultaneous presence of high amounts of OClO and NO_2, a feature which is not in line with chemical theory as shown from model calculations. Secondly, when remote-sensing observations of NO_2 from balloon and satellite are adequately compared to in situ data significant differences are

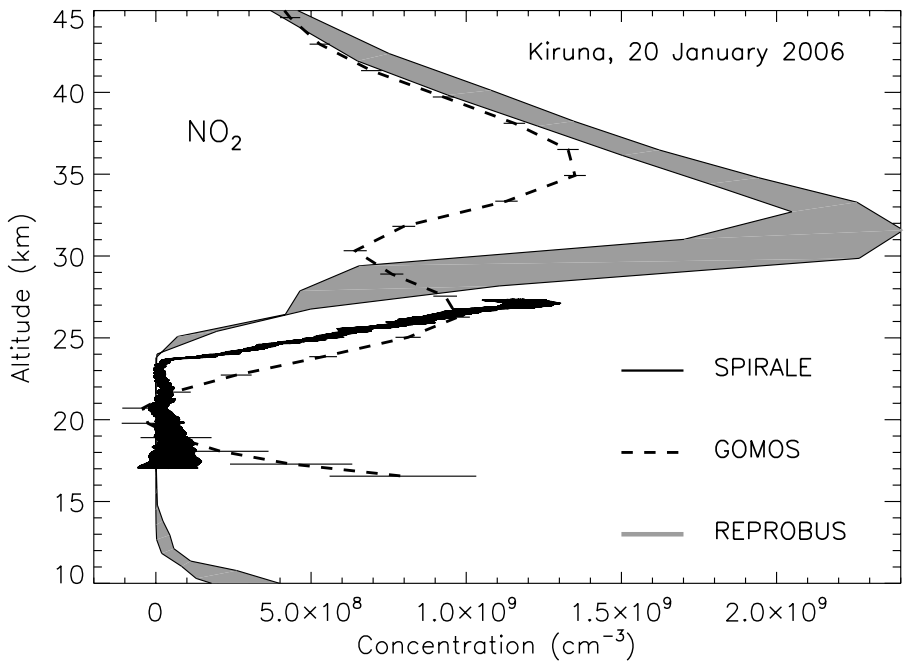

Figure 4. Vertical profile of NO_2 from nighttime in situ observations of SPIRALE (around 67.7°N–21.6°E) inside the polar vortex on 20 January 2006 (1800–1950 UT). The profile is compared to the GOMOS/Envisat measurements available close to the balloon observations. Also represented are the REPROBUS model calculations as in Figure 2 (shaded area). The thickness of the SPIRALE curve is due to both the high vertical resolution and the error bars.

clearly apparent in the lower stratosphere. The in situ measurements do not confirm the high amounts of NO_2 observed by the remote-sensing instruments in air masses expected to be denoxified in the winter polar vortex conditions. These two points together give a hint that remote-sensing observations may generate artificial structures at least for altitude levels in the lower stratosphere. The role of spatial inhomogeneities in the atmospheric layers sounded by SALOMON and GOMOS is strongly suspected.

4.3. Hypothesis of Spatial Homogeneity

4.3.1. Dynamical Situation

[23] To investigate the hypothesis of spatial homogeneity, let us focus on the GOMOS and REPROBUS profiles at altitudes above the balloon measurements. NO_2 amounts are usually strongly variable with the altitude depending on the strength of the vortex and on the involved chemical processes. In Figure 3, the enhancement visible between 35 and 40 km in both REPROBUS and GOMOS profiles appears to be the result of perturbed dynamical conditions. From the Potential Vorticity (PV) map at 950 K (about 32 km) calculated by the MIMOSA advection contour model [*Hauchecorne et al.*, 2002], commonly used to analyze the dynamical conditions encountered during balloon flights [*Huret et al.*, 2006], it seems that some of the ascent lines of sight of SALOMON cross a PV blob reaching the core of the vortex at this level and corresponding to lower PV values than the surrounding vortex air masses (Figure 5). This is likely the signature of extra-vortex air intrusion. The air at stratospheric levels above the balloon float altitude probably experienced significant mixing with NO_2-rich air drawn from midlatitudes which manifests itself as the enhancement in NO_2 amounts in the 35–40 km altitude range. The NH polar vortex is often asymmetric and vertically distorted away from the North Pole position resulting in the presence of air advected from midlatitudes to latitudes close to the pole. This was also the case at the time of SPIRALE observations for levels above SPIRALE float altitude as revealed by the large peaks above 30 km in GOMOS observations, in the REPROBUS model and also by MIMOSA PV fields (Figure 6).

4.3.2. Slant Column Densities

[24] Figure 7 presents the NO_2 SCDs observed by SALOMON during the ascent of the balloon and at float altitude. It must be noted that these SCD values are obtained relatively to the contribution of NO_2 absorption in the reference spectrum considered however to be weak (such contribution is visible as an offset of the whole SCD profile). A flight configuration with positive moon elevation angles provides measurements more sensitive to small scale concentration variations than a typical occultation. At float during a moon set or a moon rise below the gondola horizon, the stratospheric part of the lines of sights reaches several hundred of kilometers contrasting with the several tens of kilometers for an ascent configuration. This gives the possibility of emphasizing the local variations of the species concentrations resulting from the dynamical disturbance. Strong small-scale NO_2 oscillations are clearly visible in the ascent pattern of the SCDs in Figure 7. After a careful examination, such SCD fluctuations are not found to be the result of vertical variations or jolts in the balloon trajectory which is rather smooth and monotonic, or simply due to the evolution of the observation geometry (variations of optical paths in the atmospheric layers as the balloon and moon are

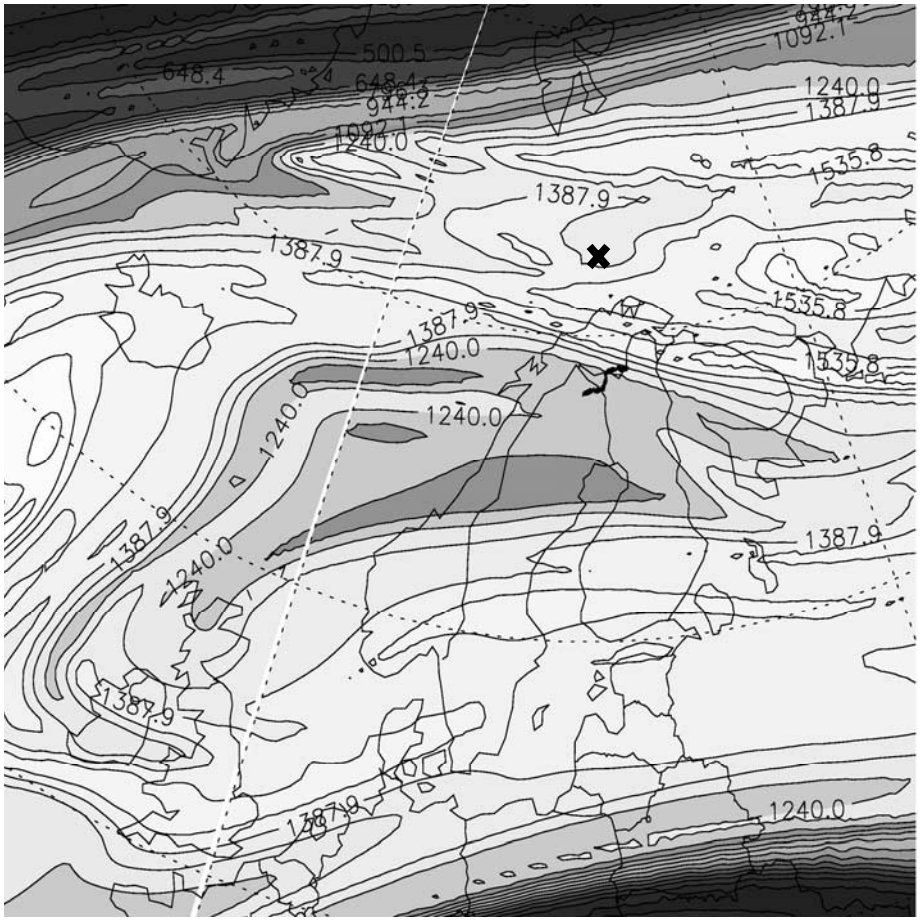

Figure 5. Potential Vorticity isocontours in pvu (1 pvu = 10^{-6} m^2 s^{-1} kg^{-1} K) calculated by the MIMOSA high-resolution model at 950 K (about 32 km) on 16 January 2006 at 1800 UT. The positions where the lines of sight of SALOMON intersect this level are also shown (bold black line above Scandinavia). GOMOS measurement positions are also shown (thick cross).

rising). The SCD enhancements are superimposed on the rather monotonic SCD trend that one would expect considering the geometry of observation (increasing positive moon elevation angles, displacement of the balloon) and the typical spatial variation of stratospheric NO_2. Then these fluctuations, also observed at float (considering that the balloon altitude at float only slightly varies), appear to be the signature of the small-scale variations in the NO_2 amounts in the atmospheric layers intersected by some lines of sight as the balloon position varies. This directly reflects the non-uniformity of the layers. In other words the hypothesis of homogeneity is not achieved for the retrieval of NO_2 as a result of the dynamical effects described above.

[25] The examination of the NO_2 SCD profiles obtained by GOMOS on 16 and 20 January 2006 coincidently to SALOMON and SPIRALE observations confirms this situation (Figure 8). The two profiles show very similar features with some strong enhancements at and below about 35 km tangent height, with however a smoother trend above 35 km on the 20 January data. In a situation of NO_2 concentration uniformity and considering the setting star geometry of observation the GOMOS SCD profile should vary more monotonically. The SCD enhancements around 25–27 km in Figure 8 are due to the concentration maximum of NO_2 typically located at these altitude levels. The concentration maximum located around the 35 km altitude level (Figures 3 and 4) results from the SCD bump clearly present at the corresponding tangent height in Figure 8 and is believed to be the imprint of NO_2-rich air intrusions along the GOMOS lines of sight as for the SALOMON case. The NO_2 maximum at 35 km resulting from this intrusion is apparently not crossed by the GOMOS lines of sight corresponding to lower tangent heights. The validity of spatial homogeneity is therefore ruled out in these two cases of GOMOS observations. Note that unlike SALOMON observations, small NO_2 variations cannot be emphasized from the observation geometry of GOMOS due to the longer lines of sight.

[26] Note that to explain the NO_2 SCD enhancements shown in Figure 7 one could have suspected an effect of energetic particle precipitation events similar to those recently observed by satellite instruments over southern and northern polar hemispheres [e.g., *Randall et al.*, 2005; *Funke et al.*, 2005; *Renard et al.*, 2006]. Precipitating solar protons and electrons are able to produce large quantities of NO_x in the mesosphere with subsequent descent to the upper stratosphere. For instance, pronounced enhancements in the vertical column density of NO_2 were observed by the

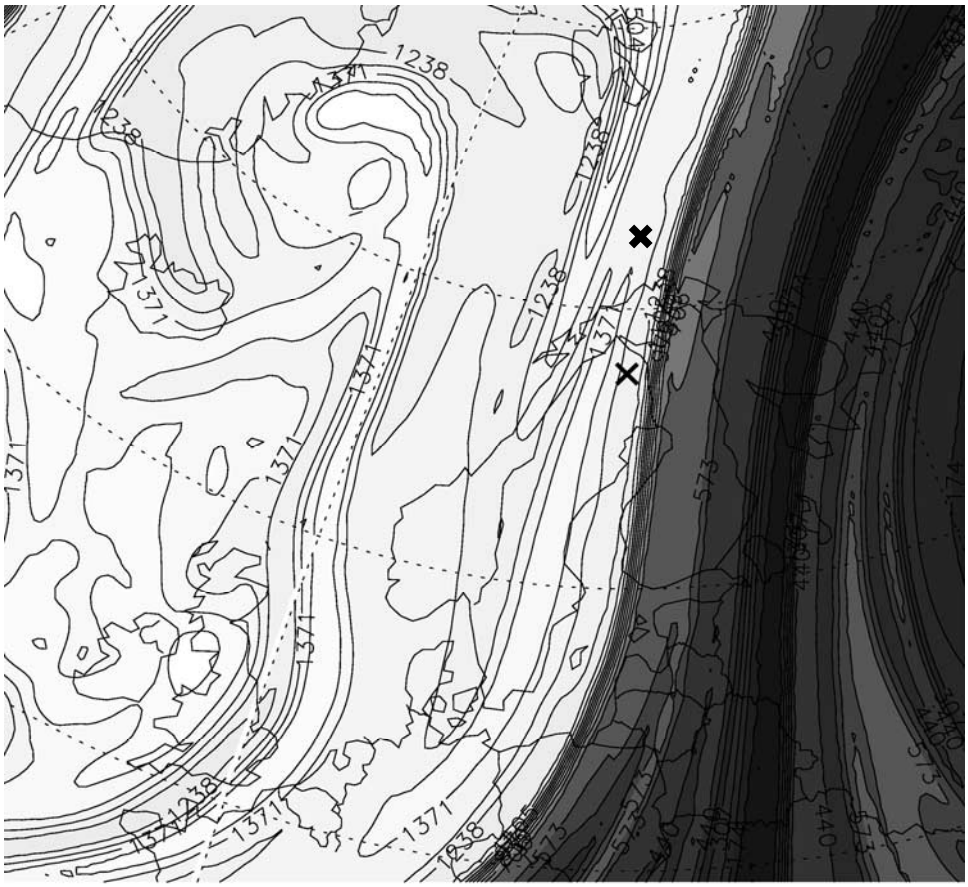

Figure 6. PV isocontours in pvu (1 pvu = 10^{-6} m^2 s^{-1} kg^{-1} K) calculated by the MIMOSA high-resolution model at 950 K (about 32 km) on 20 January 2006 at 1800 UT. Note the position (black cross) of SPIRALE observations below this level. GOMOS measurement positions are also shown (thick cross).

SAOZ ground-based UV-visible spectrometer in January 2004 above Sodankyla (Finland) and were associated with precipitating particles [*Renard et al.*, 2006]. In this case a concentration maximum of NO_2 was detected by the GOMOS and MIPAS instruments at an altitude of about 60 km. Depending on the coverage and horizontal repartition of these events they may corrupt the hypothesis of homogeneity of the layers crossed by the lines of sight of a remote-sensing instrument. In the January 2006 cases studied in this paper no mesospheric NO_x productions were detected.

[27] Figure 9 shows the SCD values of OClO measured by SALOMON. It clearly comes out that OClO SCD pattern presents significant variations resulting from the different natures of air masses crossed by the lines of sight, as for NO_2. However, the general trend is different. In Figure 7 NO_2 SCDs generally decrease as the moon elevation angle rises whereas OClO SCDs decrease only between 6 and 10°. For higher elevation angles, minimum OClO SCD peaks are close to zero. They can be explained by the midlatitude originating air masses fully lacking in OClO that are present above the balloon float altitude. The lines of sight cross either these OClO-deprived air masses or OClO-rich (and chlorine active) vortex air masses. OClO-deprived air masses may be in chlorine active regions of the stratosphere yet, due to the different solar zenith angle (SZA) dependences of the photolysis efficiencies of BrCl (the nighttime reservoir of BrO) and OClO [*Canty et al.*, 2005]. Some peaks in Figure 9 can be related to the history of the vortex air masses which can significantly impact the OClO quantities observed at the time-position of the balloon flight.

[28] We focus now on the SALOMON SCDs obtained at float altitude. In this case the displacement of the balloon is quasi-horizontal and the SCDs are not used for the retrieval of the vertical profile. However, they can be useful to test the consistency of the SALOMON observations toward chemical theory in a geometry of observation corresponding to an air mass number lower than for ascent. Figure 10 presents the fluctuations of the differential SCDs both for NO_2 and OClO observed by SALOMON around float altitude. Differential SCDs represented in Figure 10 have been obtained after applying a high-pass filtering procedure allowing the removal of low frequencies (in particular the general trend of each SCD profile). With this procedure only the fluctuations of the NO_2 and OClO SCDs become apparent and can be adequately compared. A NO_2-OClO SCD anti-correlation is clearly apparent in Figure 10 with opposite features sharply varying from a line of sight to another, in close locations, while one would expect a rather steadily varying trend between NO_2 and OClO SCDs in presence of predominantly uniform layers. A NO_2-OClO

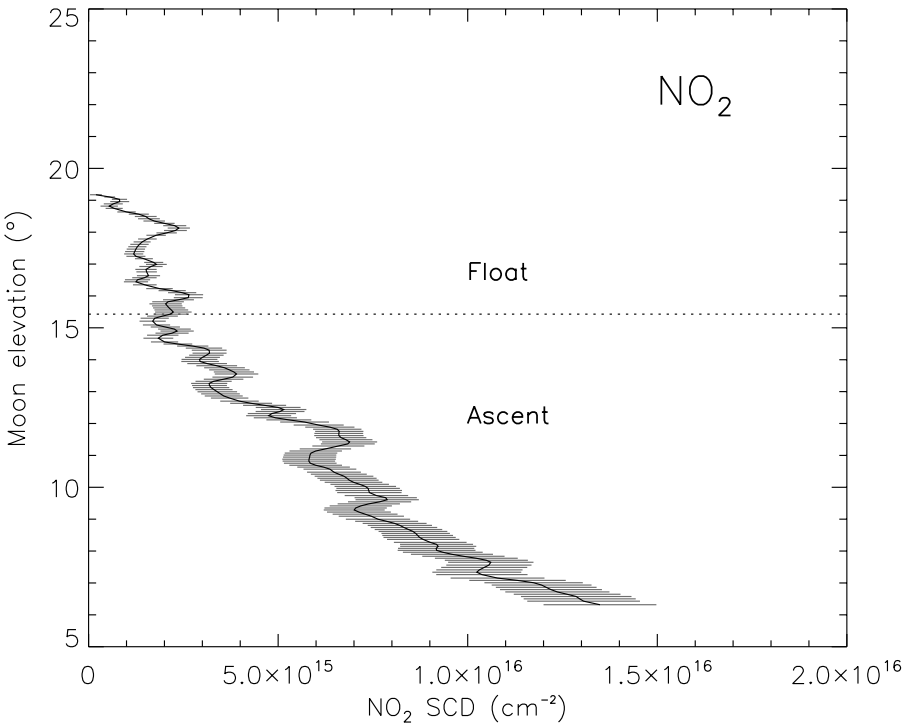

Figure 7. NO_2 SCDs measured by SALOMON for varying moon elevation angles during the balloon ascent and at float altitude (about 33 km). Note that the SCD value at 19.5° corresponds to the spectrum used as reference.

anti-correlation in the SCDs is consistent with the chemical mechanism involving these two species. This is totally in opposition with the conclusions directly inferred from the vertical profiles of NO_2 and OClO (calculated using the SCDs observed during ascent) suggesting simultaneous presence of significant quantities of these two species.

4.3.3. Vertical Profiles

[29] Such variability in the SCD profiles is liable to affect the vertical profile retrieval from the SALOMON ascent

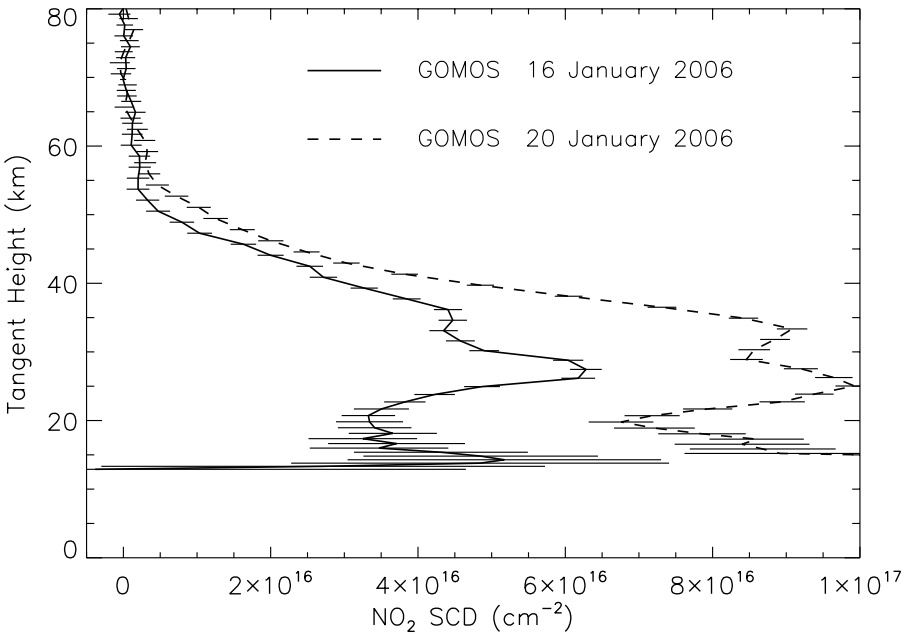

Figure 8. GOMOS SCD values of NO_2 (cm^{-2}) versus line-of-sight tangent height (km) obtained on 16 January 2006 coincidently to SALOMON observations and on 20 January 2006 coincidently to SPIRALE observations. The profiles have been sliding-averaged over 3 points.

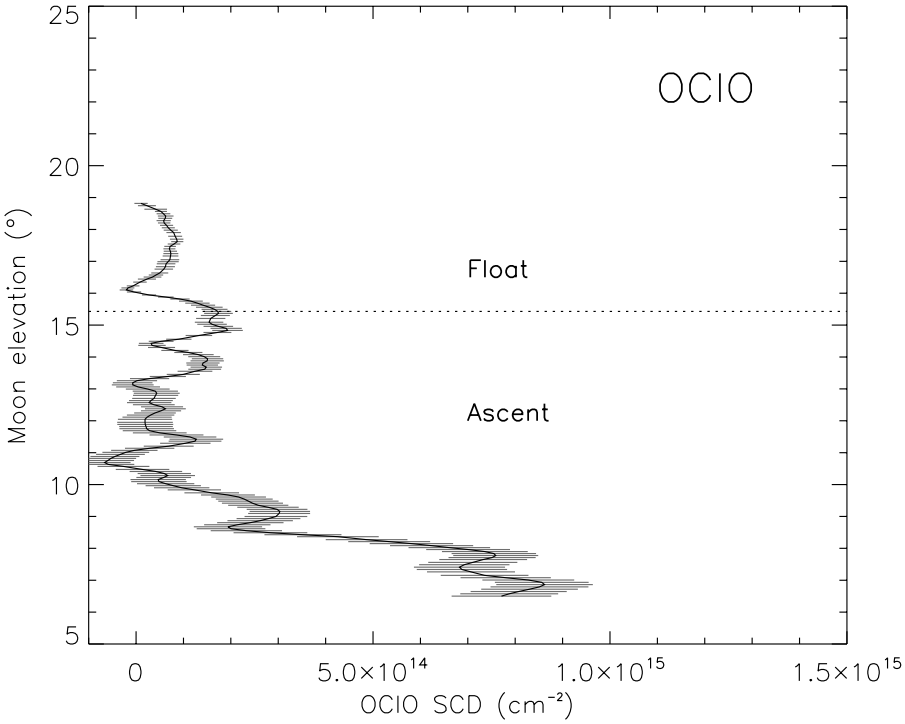

Figure 9. Same as Figure 7 but for OClO.

observations (and subsequently biasing the conclusions inferred from the simultaneous studies of NO_2 and OClO) when using the spatial least squares inversion that assumes spatial homogeneity. Such method is known to be sensitive to local fluctuations. It is then worth to determine the extent of this effect on the vertical profile retrieval and to try to minimize it. We have performed a qualitative test consisting in fitting the ascent NO_2 SCD profile using polynomials. As a second step the mathematical inversion of the SCD profile fit has been carried out. The process has been reiterated until a satisfactory minimization of the concentration values of NO_2 is achieved in the lower stratosphere part of the profile consistent with SPIRALE in situ data and model calculations. Two fits obtained using second-order polynomials are presented in Figure 11. One fit mainly passes through or closely to the minimum values of the SCDs. The newly calculated vertical profile inferred from this fit and shown in Figure 12 clearly reveals NO_2 concentration values lower

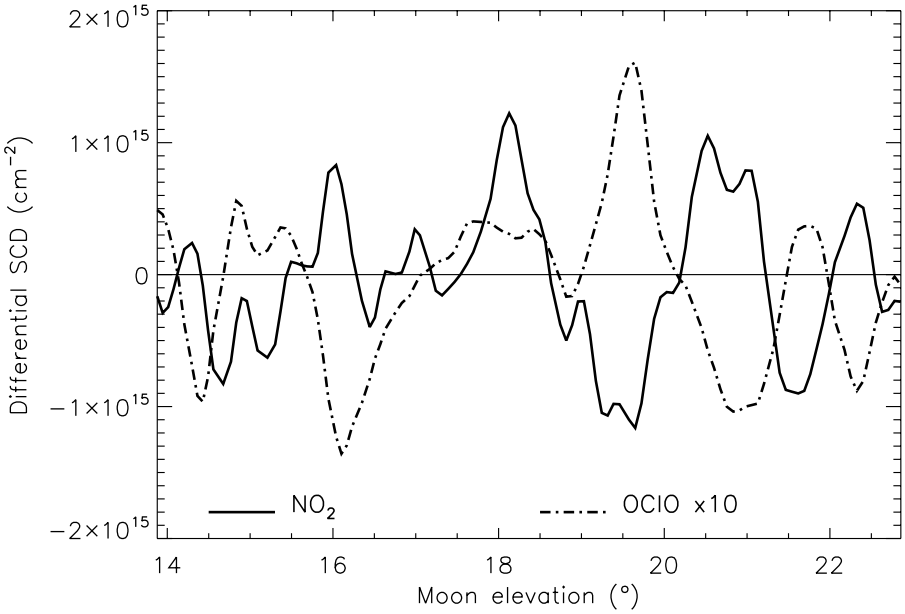

Figure 10. Evolution of the differential SCDs of NO_2 and OClO measured by SALOMON around the balloon float altitude. OClO SCDs have been multiplied by 10 for clarity.

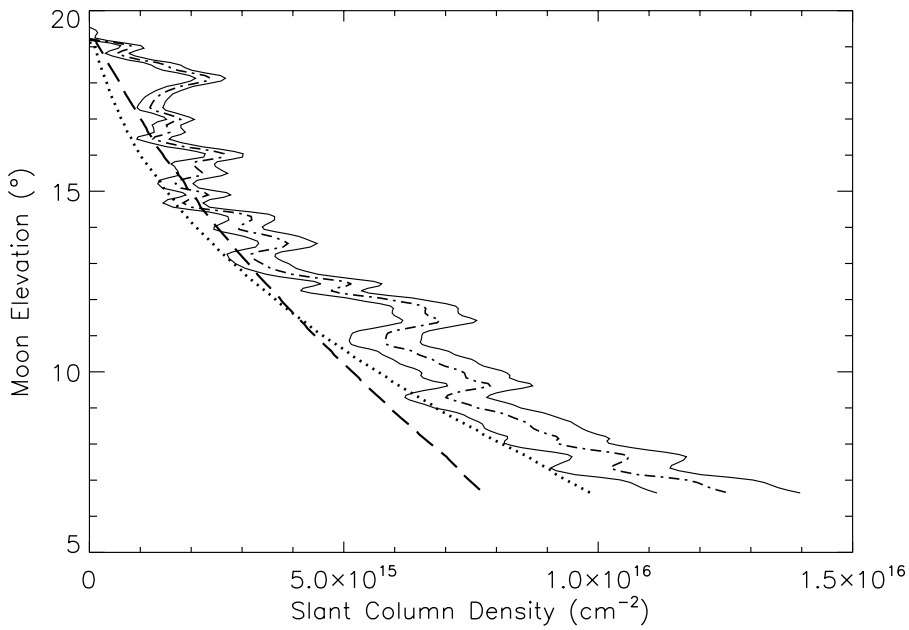

Figure 11. NO_2 SCD profile (including error range) versus moon elevation obtained during the SALOMON balloon ascent together with two fits using second-order polynomials (dashed and dotted lines). The fits are used to calculate concentration values minimized in the lower stratosphere as shown in Figure 12.

than in the initial SALOMON vertical profile and closer to the in situ observations below 23 km. Better agreement is also obtained with the simulated amounts of NO_2 at these altitudes and in the 26–29 km altitude range. The other polynomial fit shown in Figure 11 exhibits a negative bias below 13° elevation angle but interestingly results in NO_2 concentration values close to zero below 23 km which better capture the in situ observations. This straightforward test reveals the impact of the NO_2 SCD enhancements on the retrieved vertical profile but it does not allow us to remove accurately their contribution.

[30] The OClO case is rather different. OClO amounts simulated above 33 km are a factor of ~10 below the maximum values at 20 km (Figure 2). No high altitude

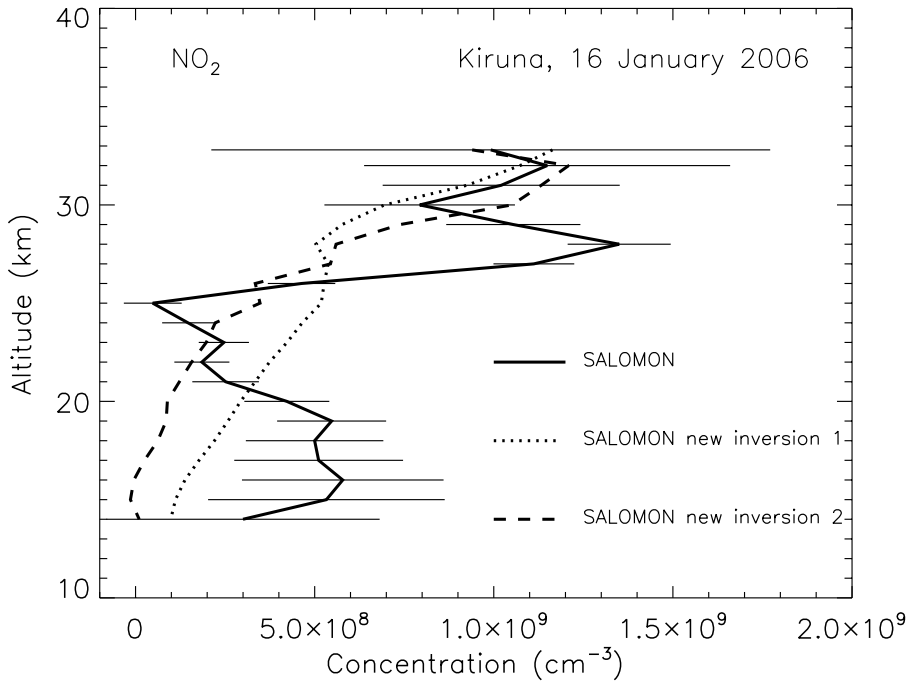

Figure 12. Vertical profiles of NO_2 obtained from the SCD test fits shown in Figure 8 (dashed and dotted lines) compared to the initial SALOMON profile (full line).

concentration enhancement is apparent in the modeled profile since intrusions of midlatitude air above the float altitude bring low amounts of OClO subsequently mixing to the OClO-abundant vortex air masses, a somewhat opposite feature to the situation for NO_2. The upper part of the OClO vertical profile corresponding to atmospheric layers closer to the dynamically perturbed levels is however characterized by large error bar seen in Figure 2. Then the OClO inhomogeneities pointed out by the differential SCDs (Figure 10) above the balloon float altitude appear to less impact the inversion process producing the whole vertical profile.

5. Conclusion

[31] The observations of three kinds of instruments, two using remote-sensing methods and one using in situ sounding of stratospheric species, have been performed in the Arctic polar vortex in similar geophysical conditions. From the intercomparison of these data, the deficient published measurement-model comparisons regarding the coupling of the chemically linked NO_2 and OClO species appear to be mainly the result of an artifact in the retrieval methods which assume spatial homogeneity. This problem mostly affects the NO_2 retrieval by recurrently generating artificial high quantities of NO_2 in the lower part of the vertical profiles obtained from the remote-sensing instruments. In the study presented here the homogeneity hypothesis is not achieved in the atmospheric area sounded by the instrument due to the perturbed dynamical conditions with presence of NO_2-rich air drawn from midlatitudes resulting in NO_2 gradients and anomalous NO_2 enhancements in the slant column density profiles. More generally, this is likely to impact occultation observations (with the light source at negative and positive elevation angles) and limb measurements from balloons or satellites, all these types of observations using inversion methods that are not robust to inhomogeneities that can be present from the lower to the upper stratosphere.

[32] Another high-latitude phenomenon may be believed to potentially spoil the hypothesis of homogeneity. Particle precipitation events have been shown to produce high amounts of NO_x at high altitudes followed by downward transport to the upper stratosphere such as in the 2003–2004 Arctic winter [*Randall et al.*, 2005; *Renard et al.*, 2006]. If lines of sight intersect those NO_2-boosted high-altitude air masses non-uniformly distributed in the layers sounded by the remote-sensing instrument, they are liable to corrupt NO_2 retrievals.

[33] Discussing the chemical processes involving the NO_2 and OClO species or more generally the interactions between nitrogen and chlorine families is out of the scope of this paper. But it is clear that analysis of these interactions or studies of the NO_y chemistry from the remote-sensing data could be biased when lines of sight cross air masses of different origins, which is potentially the case in the vicinity of the polar vortex edge (one could for example think of the HNO_3 species showing strong contrast between denitrified vortex air and extra-vortex air), depending on the occurrence of perturbed dynamical situations. The dynamical conditions must then be considered carefully which was not systematically done in some previously published studies. In the case of strong inhomogeneities, inferences drawn from relatively crude analysis of the NO_2 and OClO profiles observed in the future by remote-sensing instruments may be misleading. In this paper we present an analysis based on observations of slant column density variations over a large altitude range and at float altitude. The balloon measurements analyzed in the works of *Rivière et al.* [2002] and *Canty et al.* [2005] were not similarly investigated due to the limited altitude range of these observations. The high amounts of NO_2 published by *Rivière et al.* [2002] are difficult to understand considering the current knowledge of stratospheric chemistry. Following our results these quantities are doubtful. However, the conclusion that OClO chemistry is correctly known in denoxified conditions seems to remain valid.

[34] Next step of this work is to investigate the validity of the homogeneity hypothesis and possible consequences on vertical profiles retrieved at midlatitudes in cases of tropical air intrusions that have been shown to occur at some altitude levels.

[35] **Acknowledgments.** We would like to thank the space French agency CNES balloon launching team. The SALOMON and SPIRALE flights were founded by ESA and CNES during the Envisat validation project.

References

Bekki, S., and K. S. Law (1997), Sensitivity of the atmospheric CH_4 growth rate to global temperature changes observed from 1980 to 1992, *Tellus, Ser. B*, *49*(4), 409–416.

Bekki, S., K. S. Law, and J. A. Pyle (1994), Effect of ozone depletion on atmospheric CH_4 and CO concentrations, *Nature*, *371*(6498), 595–597.

Bekki, S., J. A. Pyle, W. Zhong, R. Toumi, J. D. Haigh, and D. M. Pyle (1996), The role of microphysical and chemical processes in prolonging the climate forcing of the Toba eruption, *Geophys. Res. Lett.*, *23*, 2669–2672.

Bertaux, J.-L., et al. (2004), First results on GOMOS/ENVISAT, *Adv. Space Res.*, *33*(7), 1029–1035.

Berthet, G., J. Renard, M. Chartier, M. Pirre, and C. Robert (2003), Analysis of OBrO, IO, and OIO absorption signature in UV-visible spectra measured at night and at sunrise by stratospheric balloon-borne instruments, *J. Geophys. Res.*, *108*(D5), 4161, doi:10.1029/2002JD002284.

Berthet, G., N. Huret, F. Lefèvre, G. Moreau, C. Robert, M. Chartier, V. Catoire, B. Barret, I. Pisso, and L. Pomathiod (2006), In situ profiles of N_2O, NO_2 and HNO_3 at mid-latitudes retrieved from the SPIRALE balloon-borne instrument, *Atmos. Chem. Phys.*, *6*, 1599–1609.

Burkholder, J. B., J. J. Orlando, and C. J. Howard (1990), Ultraviolet-absorption cross-sections of Cl_2O_2 between 210 and 410 nm, *J. Phys. Chem.*, *94*, 687–695.

Canty, T., et al. (2005), Nighttime OClO in the winter Arctic vortex, *J. Geophys. Res.*, *110*, D01301, doi:10.1029/2004JD005035.

Carslaw, K., B. Luo, and T. Peter (1995), An analytic expression for the composition of aqueous HNO_3–H_2SO_4 stratospheric aerosols including gas phase removal of HNO_3, *Geophys. Res. Lett.*, *14*, 1877–1880.

Davies, S., et al. (2002), Modeling the effect of denitrification on Arctic ozone depletion during winter 1999/2000, *J. Geophys. Res.*, *107*, 8322, doi:10.1029/2001JD000445. [printed *108*(D5), 2003]

Funke, B., M. López-Puertas, S. Gil-López, T. von Clarmann, G. P. Stiller, H. Fischer, and S. Kellmann (2005), Downward transport of upper atmospheric NO_x into the polar stratosphere and lower mesosphere during the Antarctic 2003 and Arctic 2002/2003 winters, *J. Geophys. Res.*, *110*, D24308, doi:10.1029/2005JD006463.

Gao, R. S., et al. (1997), Partitioning of the reactive nitrogen reservoir in the lower stratosphere of the southern hemisphere: Observations and modeling, *J. Geophys. Res.*, *102*, 3935–3949.

Hauchecorne, A., S. Godin, M. Marchand, B. Heese, and C. Souprayen (2002), Quantification of the transport of chemical constituents from the polar vortex to midlatitudes in the lower stratosphere using the high-resolution advection model MIMOSA and effective diffusivity, *J. Geophys. Res.*, *107*(D20), 8289, doi:10.1029/2001JD000491.

Hauchecorne, A., et al. (2005), First simultaneous global measurements of nighttime stratospheric NO_2 and NO_3 observed by Global Ozone Monitoring by Occultation of Stars (GOMOS)/Envisat in 2003, *J. Geophys. Res.*, *110*, D18301, doi:10.1029/2004JD005711.

Hoppel, K., R. Bevilacqua, G. Nedoluha, C. Deniel, F. Lefèvre, J. Lumpe, M. Fromm, C. Randall, J. Rosenfield, and M. Rex (2002), POAM III observations of arctic ozone loss for the 1999/2000 winter, *J. Geophys. Res.*, *107*(D20), 8262, doi:10.1029/2001JD000476.

Huret, N., M. Pirre, A. Hauchecorne, C. Robert, and V. Catoire (2006), On the vertical structure of the stratosphere at midlatitudes during the first stage of the polar vortex formation and in the polar region in the presence of a large mesospheric descent, *J. Geophys. Res.*, *111*, D06111, doi:10.1029/2005JD006102.

Knight, G., A. R. Ravishankara, and J. B. Burkholder (2002), UV absorption cross sections of HO_2NO_2 between 343 and 273 K, *Phys. Chem. Phys.*, *4*, 1732–1737.

Lefèvre, F., G. P. Brasseur, I. Folkins, A. K. Smith, and P. Simon (1994), Chemistry of the 1991–1992 stratospheric winter: Three-dimensional model simulations, *J. Geophys. Res.*, *99*, 9183–9195.

Lefèvre, F., F. Figarol, K. Carslaw, and T. Peter (1998), The 1997 Arctic ozone depletion quantified from three-dimensional model simulations, *Geophys. Res. Lett.*, *25*, 2425–2428.

Marchand, M., S. Bekki, A. Hauchecorne, and J.-L. Bertaux (2004), Validation of the self-consistency of GOMOS NO_3, NO_2 and O_3 data using chemical data assimilation, *Geophys. Res. Lett.*, *31*, L10107, doi:10.1029/2004GL019631.

Moreau, G., C. Robert, V. Catoire, M. Chartier, C. Camy-Peyret, N. Huret, M. Pirre, L. Pomathiod, and G. Chalumeau (2005), A multi-species in situ balloon-borne instrument with six diode laser spectrometers, *Appl. Opt.*, *44*(28), 1–18.

Payan, S., C. Camy-Peyret, P. Jeseck, T. Hawat, M. Pirre, J.-B. Renard, C. Robert, F. Lefèvre, H. Kansawa, and Y. Sasano (1999), Diurnal and nocturnal distribution of stratospheric NO_2 from solar and stellar occultation measurements: Comparison with models and ILAS satellite measurements, *J. Geophys. Res.*, *104*, 21,585–21,593.

Platt, U. (1994), Differential optical absorption spectroscopy (DOAS), in *Air Monitoring by Spectroscopic Techniques*, *Chem. Anal.*, vol. 127, edited by W. M. Sigrist, pp. 27–84, John Wiley, Hoboken. N. J.

Randall, C. E., et al. (2005), Stratospheric effects of energetic particle precipitation in 2003–2004, *Geophys. Res. Lett.*, *32*, L05802, doi:10.1029/2004GL022003.

Renard, J.-B., M. Chartier, C. Robert, G. Chalumeau, G. Berthet, M. Pirre, J.-P. Pommereau, and F. Goutail (2000), SALOMON: A new, light balloonborne UV-visible spectrometer for nighttime observations of stratospheric trace-gas species, *Appl. Opt.*, *39*(3), 386–392.

Renard, J.-B., P.-L. Blelly, Q. Bourgeois, M. Chartier, F. Goutail, and Y. J. Orsolini (2006), Origin of the January–April 2004 increase in stratospheric NO_2 observed in the northern polar latitudes, *Geophys. Res. Lett.*, *33*, L11801, doi:10.1029/2005GL025450.

Renard, J.-B., et al. (2007), Validation of GOMOS-ENVISAT vertical profiles of O_3, NO_2, NO_3, and aerosol extinction using balloon-borne instruments and analysis of the retrievals, *J. Geophys. Res.*, doi:10.1029/2007JA012345, in press.

Ricaud, P., et al. (2005), Polar vortex evolution during the 2002 Antarctic major warming as observed by the Odin satellite, *J. Geophys. Res.*, *110*, D05302, doi:10.1029/2004JD005018.

Rivière, E. D., M. Pirre, G. Berthet, J.-B. Renard, F. G. Taupin, N. Huret, M. Chartier, B. Knudsen, and F. Lefèvre (2002), On the interaction between nitrogen and halogen species in the Arctic polar vortex during THESEO and THESEO 2000, *J. Geophys. Res.*, *107*, 8311, doi:10.1029/2002JD002087. [printed *108*(D5), 2003]

Rivière, E. D., M. Pirre, G. Berthet, J.-B. Renard, and F. Lefèvre (2004), Investigating the halogen chemistry from the high-latitude nighttime stratospheric measurements of OClO and NO_2, *J. Atmos. Chem.*, *48*, 261–282.

Roehl, C. M., et al. (2002), Photodissociation of peroxynitric acid in the near-IR, *J. Phys. Chem.*, *106*, 3766–3772.

Rothman, L. S., et al. (2005), The HITRAN 2004 molecular spectroscopic database: Edition of 2000 including updates through 2001, *J. Quant. Spectrosc. Radiat. Transfer*, *96*(2), 139–204.

Salawitch, R. J., D. K. Weisenstein, L. J. Kovalenko, C. E. Sioris, P. O. Wennberg, K. Chance, M. K. W. Ko, and C. A. McLinden (2005), Sensitivity of ozone to bromine in the lower stratosphere, *Geophys. Res. Lett.*, *32*, L05811, doi:10.1029/2004GL021504.

Sander, S. P., et al. (2003), Chemical kinetics and photochemical data for use in atmospheric studies, *Eval. 14*, *JPL Publ. 02–25*, 334 pp., Jet Propul. Lab., Pasadena, Calif.

Sen, B., G. C. Toon, G. B. Osterman, J.-F. Blavier, J. J. Margitan, R. J. Salawitch, and G. K. Yue (1998), Measurements of reactive nitrogen in the stratosphere, *J. Geophys. Res.*, *103*, 3571–3585.

Sessler, J., M. P. Chipperfield, J. A. Pyle, and R. Toumi (1995), Stratospheric OClO measurements as a poor quantitative indicator of chlorine activation, *Geophys. Res. Lett.*, *22*, 687–690.

Stimpfle, R. M., D. M. Wilmouth, R. J. Salawitch, and J. G. Anderson (2004), First measurements of ClOOCl in the stratosphere: The coupling of ClOOCl and ClO in the Arctic polar vortex, *J. Geophys. Res.*, *109*, D03301, doi:10.1029/2003JD003811.

Swartz, W. H., J.-H. Yee, C. E. Randall, R. E. Shetter, E. V. Browell, J. F. Burris, T. J. McGee, and M. A. Avery (2006), Comparison of high-latitude line of sight ozone column density with derived ozone fields and the effects of horizontal inhomogeneity, *Atmos. Chem. Phys.*, *6*, 1843–1852.

Wetzel, G., et al. (2002), NO_y partitioning and budget and its correlation with N_2O in the Arctic vortex and in summer midlatitudes in 1997, *J. Geophys. Res.*, *107*(D16), 4280, doi:10.1029/2001JD000916.

B. Barret, Laboratoire d'Aérologie, Observatoire de Midi-Pyrénées, 14 Avenue E. Belin, F-31400 Toulouse, France.

G. Berthet, Q. Bourgeois, V. Catoire, M. Chartier, F. Coquelet, N. Huret, J.-B. Renard, and C. Robert, Laboratoire de Physique et Chimie de l'Environnement, CNRS and Université d'Orléans, 3A Avenue de la Recherche Scientifique, F-45071 Orléans Cédex 2, France. (gwenael.berthet@cnrs-orleans.fr)

A. Hauchecorne and F. Lefèvre, Service d'Aéronomie, Institut Pierre-Simon Laplace, UPMC, 4 Place Jussieu, BP 102, F-75252 Paris, France.

E. D. Rivière, Groupe de Spectrométrie Moléculaire et Atmosphérique, Université de Reims and CNRS, Bâtiment 6, Case 36, BP 1039, F-51687 Reims Cédex 2, France.